Analysis of the vienna rectifier under nonunity power factor operation

Molligoda, Devinda A.; Pou, Josep; Gajanayake, C. J.; Gupta, A. K.

2018

Molligoda, D. A., Pou, J., Gajanayake, C., & Gupta, A. (2018). Analysis of the Vienna Rectifier under Nonunity Power Factor Operation. 2018 Asian Conference on Energy, Power and Transportation Electrification (ACEPT). doi:10.1109/acept.2018.8610866

https://hdl.handle.net/10356/144551

https://doi.org/10.1109/ACEPT.2018.8610866

Analysis of the Vienna Rectifier under Nonunity Power Factor Operation

D. A. Molligoda[(1)(2)], J. Pou[(1)(2)], C.J. Gajanayake[(3)], A.K. Gupta[(3)]

[(1)]Nanyang Technological University (NTU), School of Electrical and Electronic Engineering, Singapore
[(2)]Rolls-Royce @NTU Corp Lab, Singapore
[(3)]Rolls-Royce Singapore Pte. Ltd, Singapore, 638673

***Abstract*—The Vienna rectifier is an attractive topology due to the three-level voltage generation and its simplicity compared to other converter solutions. The Vienna rectifier generates voltage and current waveforms with low distortion under unity power factor operation. However, when the reference voltages and the grid currents are not in phase, the output voltages become distorted and therefore the grid currents as well. This paper evaluates the distortions produced due to nonunity power factor operation in the Vienna rectifier. It also discusses on possible solutions to mitigate the problem and evaluates their effectiveness and limitations.**

Keywords—Vienna rectifier; zero crossing distortion; nonunity power factor

I. INTRODUCTION

The Vienna rectifier is a three-phase, three-level converter, which topology is shown in Fig. 1. It is integrated by a diode bridge rectifier and bidirectional switches that can connect each leg of the converter to the neutral point of the dc-link capacitors. The maximum voltage that the bidirectional switches have to withstand is half the dc-link voltage. The Vienna rectifier is popular among designers due to the various advantages such as simple circuit structure, unity power factor operation, low harmonics in the grid currents, and low blocking voltage stress on the bidirectional switches [1]. The Vienna rectifier is similar to the T-type converter but with fewer active switches, thus a simplified topology. As a result, it can only transfer power in one direction, from the ac side to the dc side. The Vienna rectifier can achieve higher efficiency than a six-switch active rectifier and it also requires smaller filter inductances [2].

Although the Vienna rectifier is a three-level converter, only the neutral point connection is fully controlled through the bidirectional switches. The positive and negative voltage levels of the converter are decided by the current direction. If there is no phase displacement angle between the reference voltage and the input current, the desired voltage is generated at the input of the converter. However, if there is a certain phase displacement angle and no special action is taken, the voltage pulses generated by the converter will have opposite polarity during the intervals where the reference voltage and input current have different signs. This produces low-frequency voltage distortion, which deteriorates the grid current significantly. Even when operating at unity power factor at the grid side (Fig. 1), the Vienna rectifier does not operate at unity power factor because of the filter inductors that cause a phase displacement angle between the current and voltage waveforms. Therefore, because of this displacement angle, current distortion will be appreciated

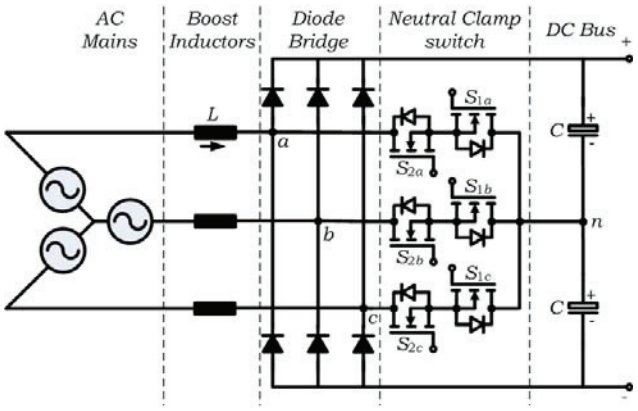

Fig. 1.The Vienna rectifier.

around the zero crossings [3]-[8]. Such distortion in the grid currents is not desired because it may violate the grid codes.

Clamping to the neutral point the leg that produces pulses with opposite sign was proposed in [3],[5]. As a result, the current distortion is significantly reduced. The duration of the clamping periods depends on the displacement angle and may last for a few switching cycles. The clamping periods help to mitigate voltage and current distortion, however they do not eliminate the low-frequency distortion completely and they have a negative effect on the voltage balancing of the dc-link capacitors. Therefore, the clamping periods should be minimized as much as possible. In [5], the authors used a fixed clamping angle, which was obtained experimentally. This would require a number of experiments for the different operation conditions. An analytical approach is discussed in [6] in which the clamping angle is calculated in an application where the Vienna rectifier is fed with a permanent magnet synchronous generator (PMSG). The current ripple due to the pulse-width modulation (PWM) is calculated and the maximum angular displacement of the current space vector in comparison to the fundamental voltage is used to find the required clamping angle.

Injecting a zero sequence into the reference signals to reduce the zero crossing distortion is discussed in [7]. A third harmonic is injected, which helps to make the duty cycles zero near the current zero crossings. But this does not solve the problem completely as still there would be some distortion due to the insufficient clamping time. The authors have extended the clamping time using redundant vectors in the space-vector PWM diagram. In [8], the reason for the zero crossing waveform distortion is analyzed using space vector modulation. A zero sequence is injected such that the leg is clamped to the

neutral point during the intervals of current-voltage with different polarity and perform a lagging reactive power compensation by using a calculated reactive current reference.

In this paper, the current zero crossing distortion problem associated with the phase displacement in the Vienna rectifier is analyzed in detail and some solutions are discussed and compared.

The paper is organized as follows. Section II presents the operation of the Vienna rectifier showing the problems associated to nonunity power factor operation. Section III introduces and compares some mitigation strategies. Finally, Section IV summarizes the main conclusions of the paper.

II. Basic Operation of the Vienna Rectifier

Fig. 2 represents a simplified single-phase diagram of a grid-connected Vienna rectifier. Synchronization with the grid voltages is performed measuring the grid voltages at Point A in Fig. 2. The phasor diagram when operating with unity power factor at the grid side is represented Fig. 3.

In this study, the converter is fed from an ideal voltage source. In practical applications, the model of the voltage source will include some impedances, however they are usually very small compared with the impedance offered by the filter inductor L.

The phase angle φ in Fig. 3 will depend on the filter inductance, the fundamental frequency and the grid current magnitude. Simulation parameters for the Vienna rectifier system are given in Table I.

First, both of the neutral point clamp switches (S_{1x}, S_{2x}) receive the same gate pulses based on the following logic:

$$S_{1x} = S_{2x} = 1, \text{ if } v_{carr1} < v_{refx} \le v_{carr2} \quad (1)$$

where $x=\{a, b, c\}$, v_{refx} is the reference signal, and v_{carr1} and v_{carr2} are the lower and upper carrier signals, respectively.

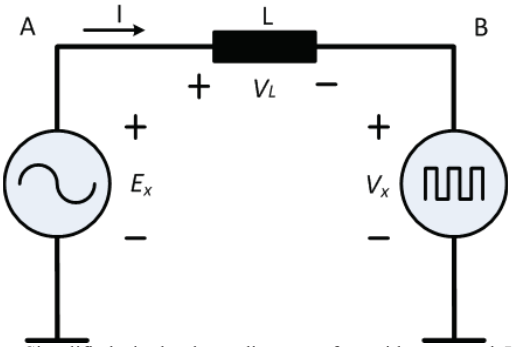

Fig. 2. Simplified single-phase diagram of a grid-connected Vienna rectifier.

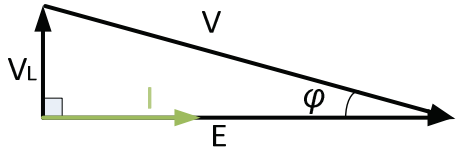

Fig. 3. Phasor diagram operating with unity power factor at the grid side (Point A).

TABLE I
Simulation Parameters

Parameter	Value
Filter inductor, L	5 mH
Line-to-line input voltage, $V_{L\text{-}L}$	400 V
DC-link output voltage, V_{dc}	800 V
Output power	12.8 kW
Output capacitor	750 uF
Fundamental frequency, f	50 Hz
Switching frequency, f_s	10 kHz

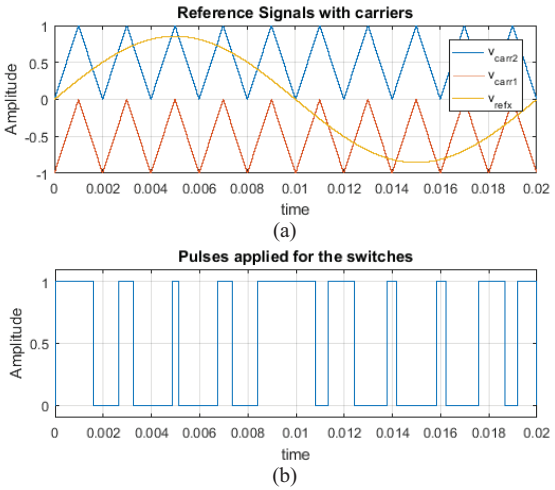

Fig. 4. Both switches controlled with the same pulses. (a) Reference signal with carriers (b) Pulses applied to the switches

Fig. 4 depicts the PWM generation for the neutral point clamp switches of one phase, using the reference signal and the two carriers. The pulses for the switches shown in Fig. 4(b) are obtained using (1).

For the sake of simplicity, let's consider a single leg in the Vienna rectifier (phase a). When the reference voltage is in the positive half-cycle and the current is positive, if none of the switches is on, the diode D_{2x} conducts and hence the voltage v_{xn} is positive (Fig. 5(a)). However, if under the same positive reference voltage the grid current is negative, the diode D_{1x} conducts and v_{xn} becomes negative, as shown in Fig. 5(c).

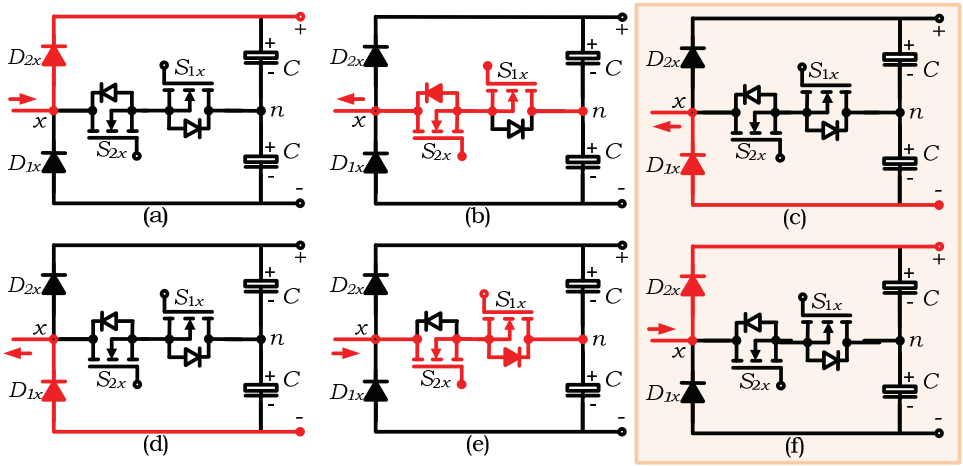

Fig. 5. Different states of a phase-leg. (a) Positive half-cycle with positive current, (b) positive half-cycle with negative current, (c) positive half-cycle with negative current (negative voltage pulse), (d) negative half-cycle with negative current, (e) negative half-cycle with positive current, and (f) negative half-cycle with positive current (positive voltage pulse).

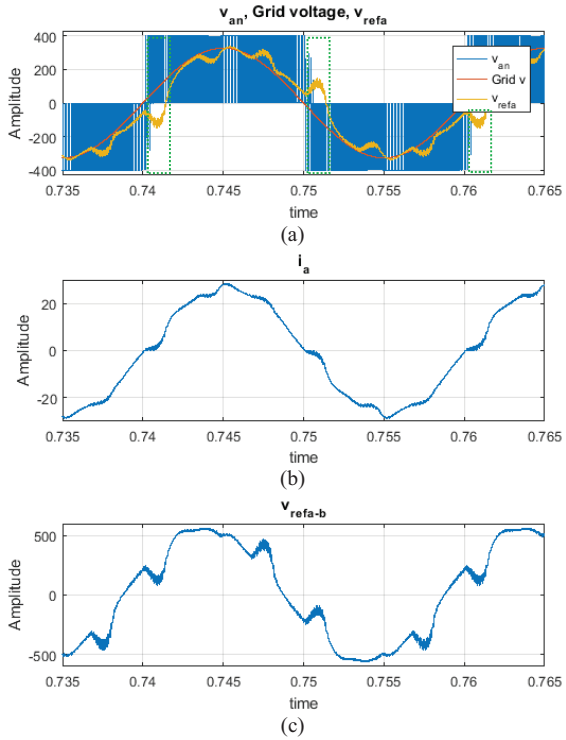

Fig. 6. Both switches controlled with the same pulses. (a) Grid voltage (Point A), converter input voltage (Point B), and reference voltage of the converter v_{ref} (b) grid current and (c) line-to-line reference voltage ($v_{refa\text{-}b}$= v_{refa}-v_{refb}).

Similarly, a positive voltage pulse will be created during the negative half cycle. As it can be observed, when both transistors are off, the voltage produced by the converter depends on the direction of the grid current. This is reasonable because the converter performs as a diode rectifier under such conditions. As a result, the voltage produced by the converter will not be the desired one when the reference voltage and the grid current have opposite signs.

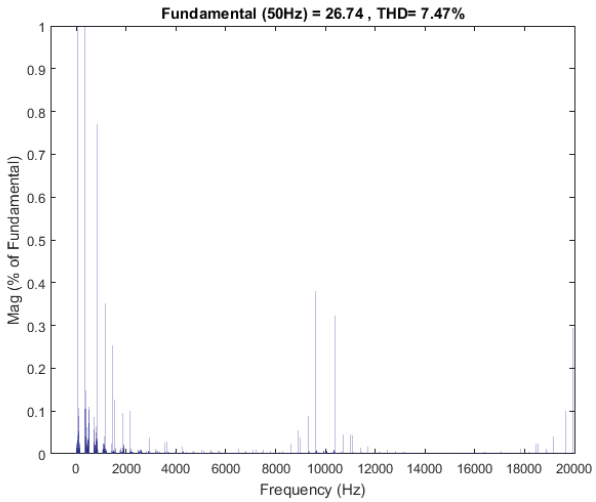

Fig. 7. Current spectrum of the grid-connected Vienna rectifier.

Fig. 6 shows the main waveforms under this operation mode. Table I indicates the main parameters of the simulation. The phase displacement angle in this test conditions is 7.78 degrees. As it can be observed in Fig. 6, despite operating with unity power factor at the grid side (Point A), there is a phase angle displacement between the reference voltage and the current at the converters side.

As a consequence, the output voltage of the converter becomes distorted. This is due to the fact that the current direction will define the polarity of the voltage pulses when the neutral point connection is not activated, producing pulses with opposite polarity during some intervals near zero crossing of the current (depicted in Fig. 6(a) with green dotted boxes).

Fig. 7 shows the current spectra. It can be observed that there is some low-frequency distortion as a result of such operation mode of the converter. The total harmonic distortion (THD) under such conditions is 7.47%.

III. Distortion Mitigation Methods

A. Clamping to the Neutral Point

In this method, the two neutral point switches receive different pulses and they are generated as shown in Fig. 8 using the following control strategy:

$$S_{2x} = 0 \text{, when } v_{refx} > v_{carr1} \text{ and } v_{refx} > v_{carr2} \quad (2)$$

$$\text{else } S_{2x} = 1$$

$$S_{1x} = 0 \text{, when } v_{refx} \le v_{carr1} \text{ and } v_{refx} \le v_{carr2} \quad (3)$$

$$\text{else } S_{1x} = 1$$

In this case, switch S_{2x} will be switching (on/off) and S_{1x} continuously on during the positive half-cycle. Similarly, in the negative half-cycle, S_{2x} will be on while S_{1x} will be switching (on/off). Using this method, the switching loss is reduced and the quality of the input currents improve.

When the converter is in the positive half cycle and the current is positive, the diode D_{2x} conducts and the voltage v_{xn} is positive (Fig. 9(a)), similar to the previous method. However, when the current is negative (Fig. 9(b)) switch S_{1x} conducts, hence clamping the output voltage to the neutral throughout the time period where the reference voltage and grid current polarities are opposite. Using the previous method, D_{1x} would conduct, generating a negative voltage in v_{xn}, which led to a negative voltage pulse in the positive half cycle, resulting in high distortion in both voltage and current waveforms.

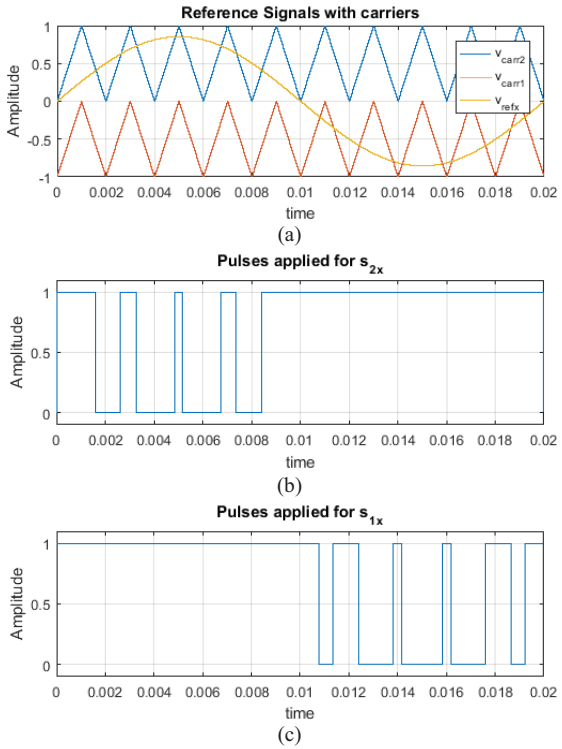

Fig. 8. Independent control of the switches. (a) Reference signal with carriers, (b) pulses applied to s_{2x}, and (c) pulses applied to s_{1x}.

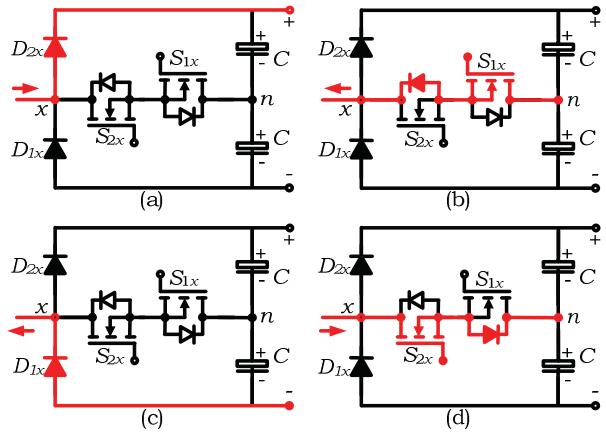

Fig. 9. (a) positive half-cycle, current positive (b) positive half-cycle, current negative (c) negative half-cycle, current negative (d) negative half-cycle, current positive.

Similarly, in the negative half cycle, when the current is negative, the diode D_{1x} conducts, and when the current is positive, the switch S_{2x} conducts, hence clamping the output voltage to the neutral point. This would avoid positive voltage pulses in v_{xn} during the negative half cycle.

Fig. 10 depicts the main waveforms when the neutral point clamp switches are given the pulses obtained using (2) and (3) under the same simulation parameters as in the previous case. Now, during the time period where the grid current and reference voltage have opposite polarities, no voltage pulses in

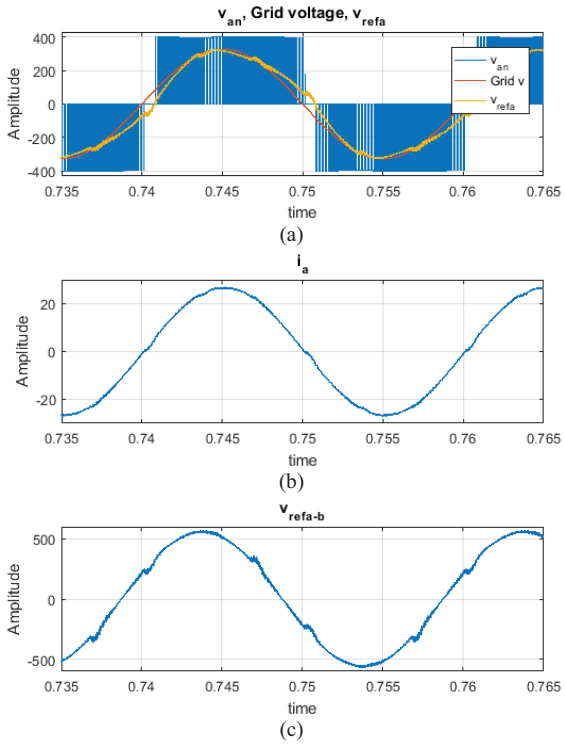

Fig. 10. Independent control of the switches. (a) Grid voltage (Point A), converter input voltage (Point B), and reference voltage of the converter v_{ref} (b) grid current, and (c) line-to-line reference voltage ($v_{refa\text{-}b}$= v_{refa}- v_{refb}).

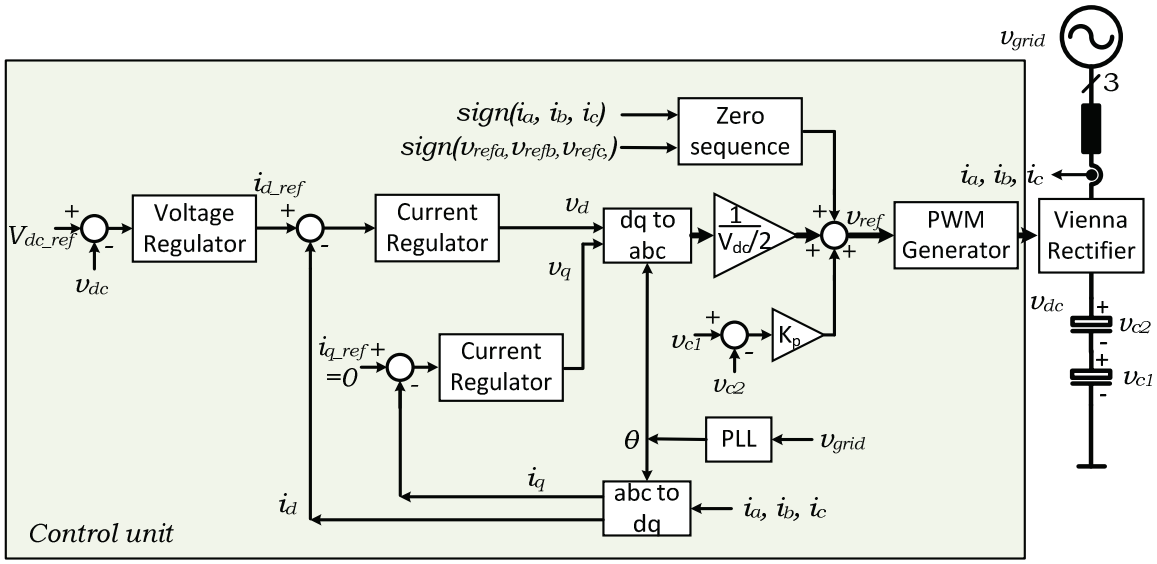

Fig. 11. Block diagram of the Vienna rectifier controller.

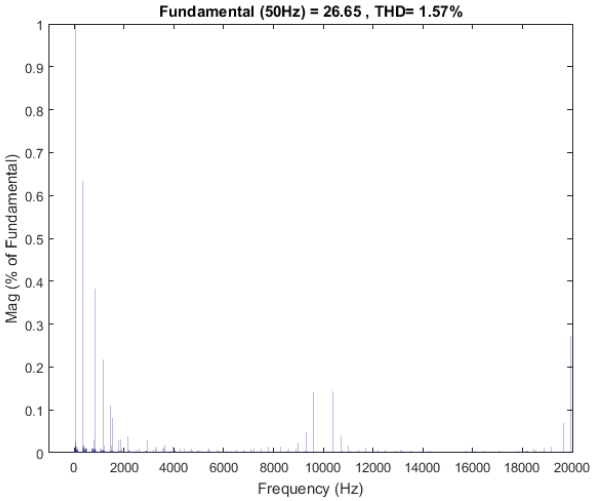

Fig. 12. Frequency spectrum of the input current when the neutral point switches are clamped during the time of opposite polarity in current and voltage.

the opposite direction appear because of the clamping to the neutral point. A grid current waveform is shown in Fig. 10(b). As it can be observed, there is a significant improvement when compared with the previous method (Fig. 6(b)). The improvement is also reflected in the current spectra shown in Fig. 12, with less low order harmonics than in the previous case (Fig. 7).

However, still during the time period where the grid current and reference voltage have opposite polarities, the line-to-line voltage becomes distorted.

B. Zero Sequence Injection

In order to completely eliminate the low-frequency distortion of the output voltage, a zero sequence can be introduced to the method described in Section III-A. This method clamps the leg to the neutral during the time period where the current and voltage polarities are opposite by forcing the reference signal for that leg to be zero. In order to avoid distortion in the line-to-line voltages, the same signal added to the reference signal for that phase is also added to the reference signals of the other phases. It is therefore a zero sequence injected into the reference signals.

The block diagram of the Vienna rectifier with voltage oriented control, including the zero sequence injection, is shown in Fig. 11. A simple proportional control is used to balance the capacitor voltages. The zero sequence is generated as follows. Compute the product of grid current and its reference voltage for all the phases and continuously check the polarity of the products. If the product is negative in a particular phase, then subtract the reference voltage of that phase from all three phases and continue until the product is positive. Repeat the above sequence for all the three phases as depicted in Fig. 13.

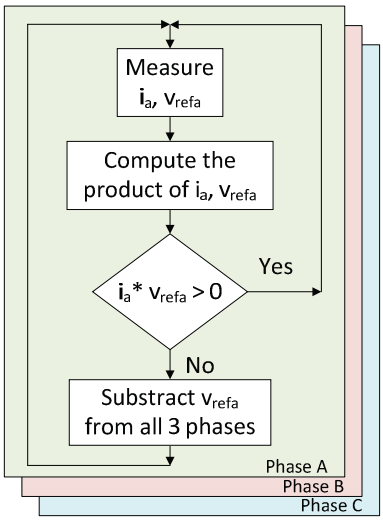

Fig. 13. Zero sequence generation.

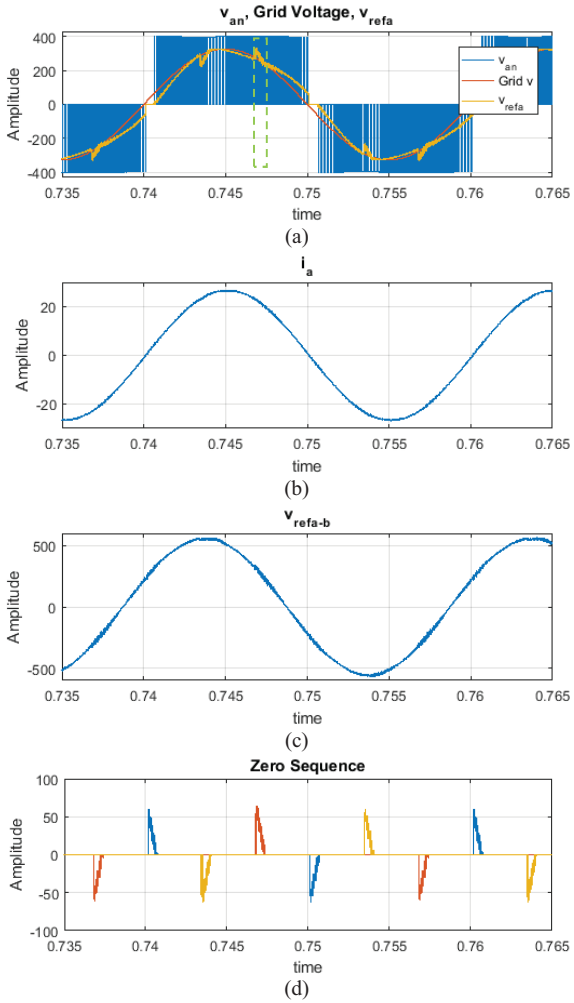

Fig. 14. Zero sequence injection. (a) Grid voltage measured at point A, converter input voltage measured at point B and reference voltage of the converter v_{refx}, (b) grid current, (c) line-to-line reference voltage ($v_{refa\text{-}b}$= v_{refa}-v_{refb}), and (d) zero sequence.

As shown in Fig. 14 and 15, once the zero sequence is injected, the line-to-line voltage distortion is reduced (Fig. 14(c)) and the THD of the input currents further reduced improving the quality of the waveforms.

However, the zero sequence injected to the reference signals (Fig. 14(a)) may produce overmodulation. Consequently, the modulation index has to be limited to avoid such overmodulation. The maximum modulation index that could be achieved depends on the phase displacement angle between the reference voltage and the input current. In order to find the maximum modulation index that can be applied without producing overmodulation, the maximum value of the reference signal once the zero sequence has been injected has to be determined. The reference signal of phase A at the time interval shown in a green box in Fig. 14(a), can be expressed as:

$$\frac{v_{refa}}{v_{dc}/2} = m[\sin\omega t - \sin(\omega t - 2\pi/3)] \qquad (4)$$

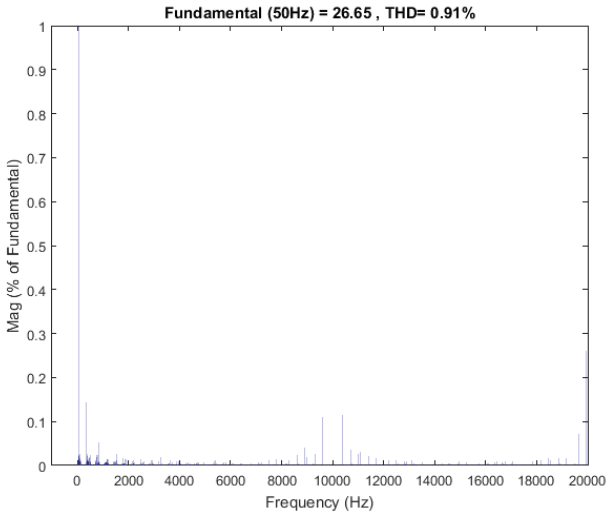

Fig. 15. Frequency spectrum of the input current when the zero sequence is injected.

where m is the modulation index ranging in the interval [0,1]. To avoid overmodulation, the maximum value from (4) cannot be larger than one, which leads to the following condition:

$$m \le \frac{1}{\sqrt{3}\sin(\pi/6 + \varphi)} \qquad (5)$$

where φ is the phase displacement angle.

The relationship between the phase angle and the maximum modulation index is shown in Fig. 16. It can be observed that the zero sequence injection is suitable for low modulation index operation. According to Fig. 16, when the phase displacement angle is less than 5.26 degrees, the modulation index can reach the unity without producing overmodulation. However, if the displacement angle is larger, the maximum modulation index is limited to a lower value, as shown in Fig. 16. Nevertheless, even if excessive zero sequence is injected and the converter reaches overmodulation, the distortion produced would be much less than in the previous cases, resulting in lower THD values.

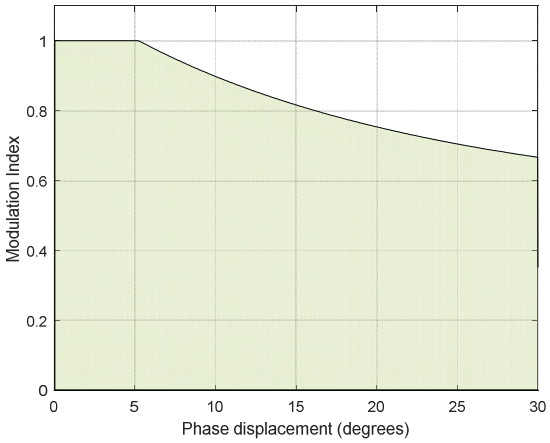

Fig. 16. Modulation index versus phase displacement angle.

COMPARISON BETWEEN MODULATION TECHNIQUES

Modulation	Simultaneous	Clamping	Zero sequence
Current THD %	7.49	1.57	0.91

Table II compares the frequency spectrums of the three cases to appreciate the improvement in the current quality. As the table shows, adding the zero sequence improves the quality of the current waveform significantly.

IV. CONCLUSION

An analysis of distortion in the current and the voltage waveforms near the zero crossing of the Vienna rectifier has been done and various methods of reducing such distortion have been discussed. By injecting a proper zero sequence to the reference signals of the Vienna rectifier, full control of the converter can be achieved, as if it was a T-type converter (with top and bottom switches instead of only diodes). However, overmodulation may be produced when operating under large modulation indices, which limits the maximum modulation index that can be applied to the converter. Nevertheless, even considering the distortion produced by overmodulation, the output voltage and current waveforms have less distortion than in the case of the other methods discussed in this paper.

ACKNOWLEDGMENT

This work is jointly funded by National Research Foundation (NRF) Singapore, Rolls-Royce Singapore Pte. Ltd, and Nanyang Technological University, Singapore.

REFERENCES

[1] J. W. Kolar, H. Ertl, and F. C. Zach, "Design and experimental investigation of a three-phase high power density high efficiency unity power factor PWM (VIENNA) rectifier employing a novel integrated power semiconductor module," in *Proc. IEEE Applied Power Electronics Conference and Exposition* (APEC), vol.2, no., pp.514-523 vol. 2, 3-7 Mar. 1996.

[2] T. Viitanen and H. Tuusa, "A steady-state power loss consideration of the 50kW VIENNA I and PWM full-bridge three-phase rectifiers," *2002 IEEE 33rd Annual IEEE Power Electronics Specialists Conference. Proceedings (Cat. No.02CH37289)*, Cairns, Qld., Australia, 2002, pp. 915-920 vol.2.

[3] T. Viltanen and H. Tuusa, "Space vector modulation and control of a unidirectional three-phase/level/switch VIENNA 1 rectifier with LCL type AC filter," in *Proc. IEEE Annual. Power Electron. Specialist Conf. (PESC)*, vol. 3, 2003, pp. 1063-1068.

[4] Houjian Xu, Wenxi Yao, and Shuai Shao, "Improved SVPWM schemes for Vienna rectifiers without current distortion," in *Proc. IEEE Energy Conversion Congress and Exposition (ECCE)* 2017.

[5] J. Alahuhtala, J. Virtakoivu, T. Viitanen, and H. Tuusa, " Space vector modulated and vector controled Vienna I rectifier with active filter function," in *Proc. IEEE Power Conversion Conf*, Nagoya, 2007, pp. 62-68.

[6] M.H. Johnson and D.C. Aliprantis, "Analysis and control of PMSG-based wind turbine with Vienna rectifier near current zero crossings," in *Proc. IEEE Power and Energy Conference at Illinois (PECI)*, pp.1-8, Feb.28-Mar. 1, 2014.

[7] W. Yao, Lv Zhengyu, M. Zhang, and Z. Lin, "A novel SVPWM scheme for Vienna rectifier without current distortion at current zero-crossing point," in *Proc. IEEE Industrial Electronics (ISIE),* pp.2349-2353, 1-4 Jun. 2014.

[8] F. Wang, Y. Teng, Z. Yuan, and J. Xu, "A maximum power factor of control algorithms of three-level Vienna Rectifier without current distortion at current zero-crossing point," in *Proc. IEEE Power Electronics and Motion Control Conference (IPEMC-ECCE Asia),* Hefei, 2016, pp. 2325-2331.